Chemical Structure of Ultrathin Silicon Nitride Films Grown by Low-Energy (0.25−5 keV) Nitrogen Implantation: An Angle-Resolved X-ray Photoelectron Spectroscopy Si 2p Study

C. Palacio* and A. Arranz

Departamento de Física Aplicada, Facultad de Ciencias, C-XII, Universidad Autónoma de Madrid, Cantoblanco, 28049-Madrid, Spain

Received: January 15, 2002; In Final Form: February 22, 2002

The reaction of N_2^+ ions with the Si(100) surface over the energy range of 0.25−5 keV has been studied by angle-resolved X-ray photoelectron spectroscopy (ARXPS) measurements of the Si 2p core levels. Position, width, and shape of the Si 2p band are explained in terms of a superposition of five components, Si^n ($n = 0$, ..., 4), which correspond to different bonding configurations denoting a Si atom with n nitrogen neighbors. The depth distribution of the different components is dependent on the ion energy. For energies below 1 keV, the surface film can be modeled by a layered film in which the composition is Si^4, Si^3, Si^2, and Si^1 in going from the surface to the substrate. Above 1 keV, a nitride film composed of a mixture of Si^1, Si^2, Si^3, and Si^4 species, with reduced Si^0 species at the near surface, was found. The differences are attributed to the effect of the ion energy on the preferential sputtering of nitrogen and on the knock-on mechanism.

Introduction

In general, the fabrication of thin film materials for technological applications is concerned with the material itself, with the interaction of the film with the substrate (i.e., the interface formation), with the growth method, and with the characterization of the film. Silicon nitride is an important material currently used as high-temperature ceramics, as a passivation layer in silicon-based microelectronics, as an insulator in thin-film transistor, as a diffusion barrier in multilayer devices, etc.[1] A number of methods to produce nitride films have been developed over the past years to improve the film quality according to the desired application. The chemical vapor deposition (CVD), in which a nitrogen-containing precursor decomposes to form a nitride on the silicon surface, or thermal reaction with nitrogen compounds has been largely used.[1,2] However, the above methods use high-temperature thermal annealing leading to unwanted side processes such as dopant diffusion, which results in the degradation of the properties of the film and coating adhesion problems.[3] A potential technique to grow silicon nitride layers is that of N_2^+ ion implantation. The general advantages of ion beam methods are the ability to modify the near surface without change of desirable bulk properties of the base material and avoidance of coating adhesion problems.[4]

From the initial efforts to systematically study the silicon nitride formation made by Taylor et al.[5] to the more recent ones of Kusunoki et al.[6] and Baek et al.,[3] the main results can be summarized as follows: Taylor et al.[5] studied the nitridation of Si using nitrogen ions at kinetic energies of 30−3000 eV and characterized the surface using X-ray photoelectron spectroscopy (XPS) and UV photoelectron spectroscopy (UPS). They proposed charge neutralization and collisional dissociation of N_2^+ as required steps for nitridation. On the other hand, position, width, and shape of the Si 2p line have been interpreted in terms of a superposition of five chemically shifted components corresponding to $Si-Si_{4-n}N_n$ ($n = 0$, ..., 4) bonding configurations,[2] being accepted that the Si−N bond nature strongly resembles that of a thermally prepared silicon nitride.[3] In addition to that, the Si surfaces nitrided with ion beams of ∼200 eV present a well-characterized film ∼1.5 nm thick on the Si substrate, but above this ion energy, the film contains nonstoichiometric compounds and many defects.[6] Finally, at higher ion energy (20 keV), the surface layer of samples implanted at a low dose is composed of a mixture of Si and Si-rich nitride regions, whereas a continuous near-stoichiometric silicon nitride is formed with increasing ion dose.[7]

However, to our knowledge, neither structural nor chemical models of the interface have been proposed until now. A powerful experimental technique to carry out this task is a photoemission study of the Si 2p core levels shifted chemically for the different bonding configurations. Furthermore, the polar-angle dependence of the intensities of these components can be used to analyze the concentration depth profiles (CDP) of the individual components, because of the decrease of the probing depth with increase of the polar angle.[4,8,9]

The purpose of this paper is to investigate the reactions of low-energy (0.25−5 keV) N_2^+ beams with clean Si(100) surfaces to characterize the reaction products and to obtain the CDP and thickness of the reacted films. The techniques of X-ray photoelectron spectroscopy (XPS) and angle-resolved X-ray photoelectron spectroscopy (ARXPS) are used in product characterization. The experimental data are quantitatively analyzed using a simple attenuation scheme and parametric models for the CDP.

Experimental Section

Si(100) single crystals (n-type, 3.5 Ω cm) manufactured by Virginia Semiconductors Inc. have been used throughout this work. The experiments were carried out in an ultrahigh vacuum chamber at a base pressure better than 6×10^{-10} Torr, rising to 2×10^{-7} Torr of N_2 during nitrogen implantation. Silicon substrates were sputter-cleaned "in situ" using a low current density 3 keV Ar^+ beam rastered over an area of 1×1 cm^2 to

* To whom correspondence should be addressed. Fax: ++34 91 3974949. E-mail: carlos.palacio@uam.es.

10.1021/jp025520q CCC: $22.00
Published on Web 03/23/2002

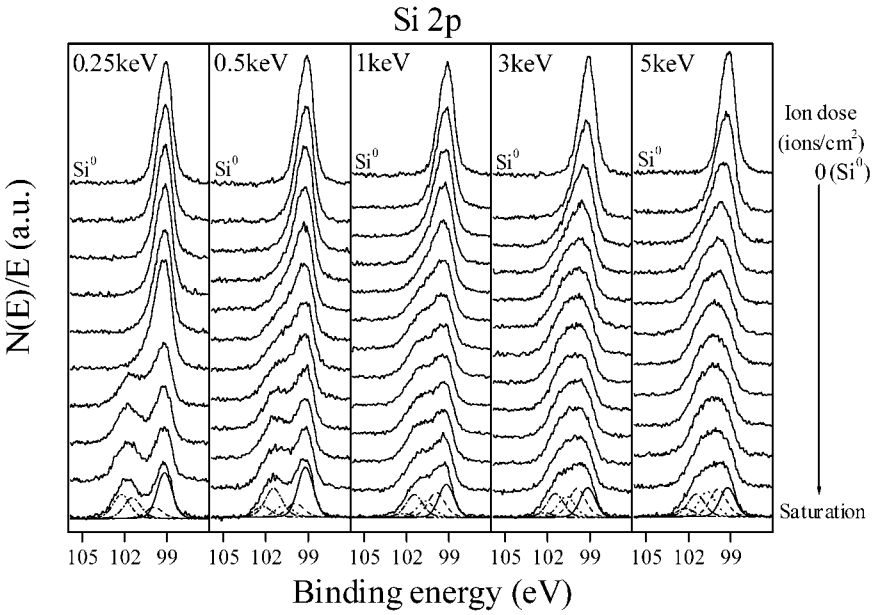

Figure 1. Progressive change of Si 2p XPS spectra from different silicon nitride layers formed by N_2^+ implantation at energies in the range 0.25−5 keV. Ion dose increases from top (0 ions/cm^2) to bottom (saturation). Examples of the deconvolution carried out with the synthetic bands Si^0, Si^1, Si^2, Si^3, and Si^4 (see text) are shown for Si 2p spectra at saturation.

minimize the development of ion-induced surface roughness until no impurities were detected by Auger electron spectroscopy (AES). Nitrogen implantation was carried out at room temperature (RT) in the ion energy (E_p) range of 0.25−5 keV. The ion beam was rastered over an area of 1 × 1 cm^2. The ion beam current density was in the range 0.1−3 μA cm^{-2} depending on the ion energy. For these experimental conditions, the ion beam composition is ∼96% N_2^+ and ∼4% N^+. The angle between the ion beam and the surface normal was 55°. XPS analysis was performed using a hemispherical analyzer (SPECS EA-10 Plus). The pass energy was 15 eV giving a constant resolution of 0.9 eV. The Ag $3d_{5/2}$ line was used to calibrate binding energies. A twin anode (Mg and Al) X-ray source was operated at a constant power of 300 W, using Mg Kα radiation. The sample was placed in a sample stage with four degrees of freedom in such a way that the takeoff angle can be varied between 0° and 70° to perform angle-resolved measurements.

Results

Figure 1 shows the evolution of the Si 2p core level spectrum of a Si(100) substrate for different ion doses up to saturation after implantation at RT by 0.25, 0.5, 1, 3, and 5 keV N_2^+ ions. Saturation ion doses are 7.9 × 10^{15}, 1.7 × 10^{16}, 4.8 × 10^{16}, 8.6 × 10^{16}, and 1.3 × 10^{17} ions cm^{-2} for 0.25, 0.5, 1, 3, and 5 keV ion energies, respectively. The background has been subtracted using a modified Shirley method.[10] The spectra labeled Si^0 are representative of the clean-sputtered Si(100) substrate. As the ion dose increases, an attenuation of the Si^0 peak and the growth in the high-binding-energy side of the Si 2p band of a new broad feature associated with the formation of silicon nitride are observed. To determine the bands associated with the different silicon species, a peak deconvolution of the spectra of Figure 1 has been carried out. The Si 2p spectra have been deconvoluted into five components, Si^0, Si^1, Si^2, Si^3, and Si,^{4} which can be attributed to clean silicon, and Si bonded to one, two, three, or four nitrogen atoms, respectively.[2,3,6] The shape of Si^0 has been obtained from the clean substrate spectrum, using an asymmetrical Gaussian−Lorentzian (GL) centered at 99.1 eV and with a full width at half-maximum (fwhm) of 1.2 eV. For the Si^1, Si^2, Si^3, and Si^4 components, symmetric GL functions of 1.4 eV fwhm and centered at 99.9, 100.7, 101.5, and 102.3 eV, respectively, have been used. These values are in good agreement with those reported in the literature.[2,3,6] They represent the minimum set of silicon components necessary to reproduce not only the spectra of Figure 1 but also the angle-resolved Si 2p spectra that will be presented later. Examples of the deconvolution are shown in the bottom of Figure 1. Here, continuous lines are used for Si^0 and dashed lines for Si^1, Si^2, Si^3, and Si^4 components.

According to Kärcher et al.,[2] the nitrogen concentration, x, of the silicon nitride, SiN_x, formed after implantation, can be calculated by eq 1,

$$x = \frac{1}{3}\left(\frac{\sum_{n=1}^{4} nI(\mathrm{Si}^n)}{\sum_{n=1}^{4} I(\mathrm{Si}^n)}\right) \qquad (1)$$

where $I(Si^n)$ stands for the XPS intensity of the Si^n component, as obtained from the deconvolution procedure.

The evolution of the N 1s core level spectra as a function of ion dose has also been measured (not shown). In all cases, only a single peak component is present in the spectra, in such a way that the N 1s spectra can be fitted well by a symmetric GL function. For a given ion energy, the binding energy of the peak center, E_o, and the fwhm increase as the ion dose increases. In addition, for a fixed ion dose, E_o and fwhm increase as the ion energy decreases. The observed dependence of E_o and fwhm values obtained from the analysis of the N 1s spectra reflects the fact that a N 1s spectrum should be a superposition of very close unresolved single peaks associated with the corresponding Si^1, Si^2, Si^3, and Si^4 species. This is supported by Figure 2, in which the evolution of E_o and fwhm of the N 1s core level is shown as a function of the nitrogen concentration, x, calculated by eq 1. The figure contains the data corresponding to all ion

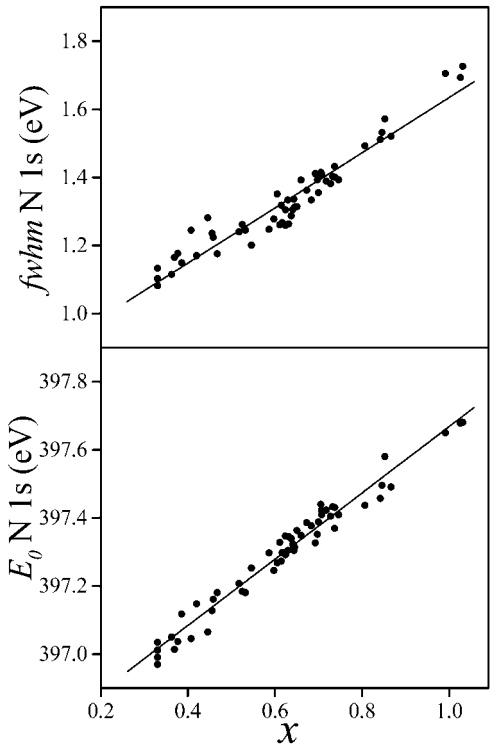

Figure 2. The binding energy, E_o, and the full width at half-maximum, fwhm, of the N 1s band as a function of the nitrogen concentration, x, of the silicon nitride, SiN_x, formed after nitrogen implantation. The figure contains the data corresponding to all ion doses and energies used in this work.

doses and energies used in this work. As can be observed, a linear dependence of E_o and the fwhm with the nitrogen concentration in the SiN_x film is found for $x \approx 0.33-1$.

Figure 3 shows the evolution of Si^0, Si^1, Si^2, Si^3, Si^4, and N XPS intensities as a function of the ion dose, for different ion beam energies. In this figure, Si^N (open circles) is the sum of all silicon nitride related species (Si^1, Si^2, Si^3, and Si^4). In the bottom of this figure, the evolution of the nitrogen concentration, x, is also shown for several ion energies as a function of the ion dose. Similar behavior for the Si^n intensities as a function of ion dose was found by Kusunoki et al.[6] during the nitridation of a Si(100) surface by 0.1−1 keV N_2^+ ion beams. Two stages can be observed for the Si^n intensity evolutions of Figure 3. In a first stage, a strong attenuation of the Si^0 signal is accompanied by the formation of Si^1 species, which increases reaching a maximum. Above this point, the Si^1 intensity slowly decreases, and the formation of Si^2, Si^3, and Si^4 species is sequentially observed with increasing the ion dose. During this second stage, a lower attenuation of the Si^0 signal is observed. In fact, for 3 and 5 keV ion beam energies, the Si^0 intensity reaches a smooth minimum, slowly increasing above the minimum with increasing ion dose. A parallel decrease of the Si^N intensity is also observed during the second stage, therefore suggesting that Si^0 reduced species are formed at the surface as a consequence of ion-bombardment-induced reduction of the SiN_x layer previously formed. At saturation, the nitride layers formed on the Si surface are nonstoichiometric compounds, SiN_x ($x \leq 1$), composed of a mixture of all Si^n components. As can be observed in the bottom of Figure 3, the ion dose necessary to reach the saturation decreases with decreasing the ion energy. In addition, below saturation, a clear dependence on the ion energy of the nitrogen concentration, x, reached at a particular ion dose is also observed. These results show that both ion energy and ion dose should be considered to obtain a complete description of the

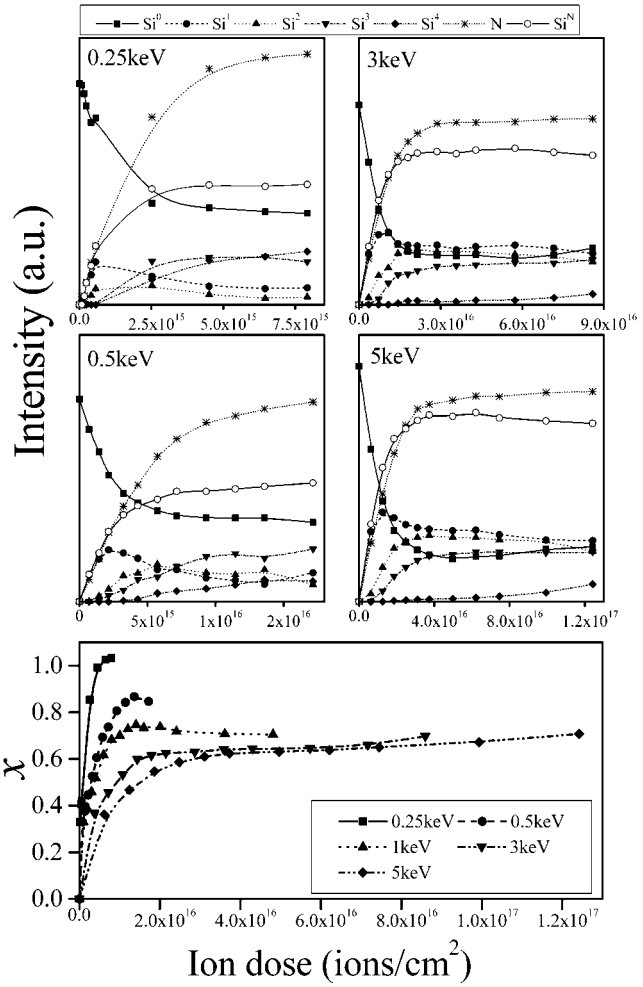

Figure 3. Intensities of the five components Si^n ($n = 0, ..., 4$), the summation $Si^N = Si^1 + Si^2 + Si^3 + Si^4$, and the N 1s band as a function of the ion dose for different ion energies. In the bottom, the evolution of the nitrogen concentration, x, of the SiN_x film as a function of the ion dose for different ion energies is also shown.

TABLE 1: Range (R_p), Range Straggling, (ΔR_p), and Si and N Sputtering Yields (S_y^{Si} and S_y^N) for N_2^+ Implantation in Si and Si_3N_4 Targets at Different Ion Energies (E_p) Calculated Using SRIM Simulations

	Si target			Si_3N_4 target			
E_p (keV)	R_p (Å)	ΔR_p (Å)	S_y^{Si} (atoms/ion)	R_p (Å)	ΔR_p (Å)	S_y^{Si} (atoms/ion)	S_y^N (atoms/ion)
5	82	44	1.17	50	27	0.60	1.35
3	56	31	1.11	34	18	0.55	1.31
2	42	24	1.03	26	14	0.51	1.19
1	26	15	0.80	16	9	0.40	0.95
0.5	17	10	0.58	11	6	0.27	0.63
0.25	11	6	0.38	7	4	0.15	0.38

kinetics of silicon nitride formation. The sputtering yields (S_y^{Si} and S_y^N), range (R_p), and range straggling (ΔR_p) for N_2^+ implantation in Si and Si_3N_4 targets, calculated using SRIM simulations,[11] are given in Table 1. According to the results of Table 1, S_y^{Si}, S_y^N, R_p, and ΔR_p decrease with decreasing ion energy. It is important to note that the sputtering yield of nitrogen in the Si_3N_4 target, S_y^N, is higher than the sputtering yield for silicon, S_y^{Si}, therefore suggesting that preferential sputtering of nitrogen in the SiN_x film already formed at intermediate ion doses should be important, above all at higher ion energies. As a general trend, Taylor and Rabalais[12] have observed a decrease of the reaction cross section with increasing

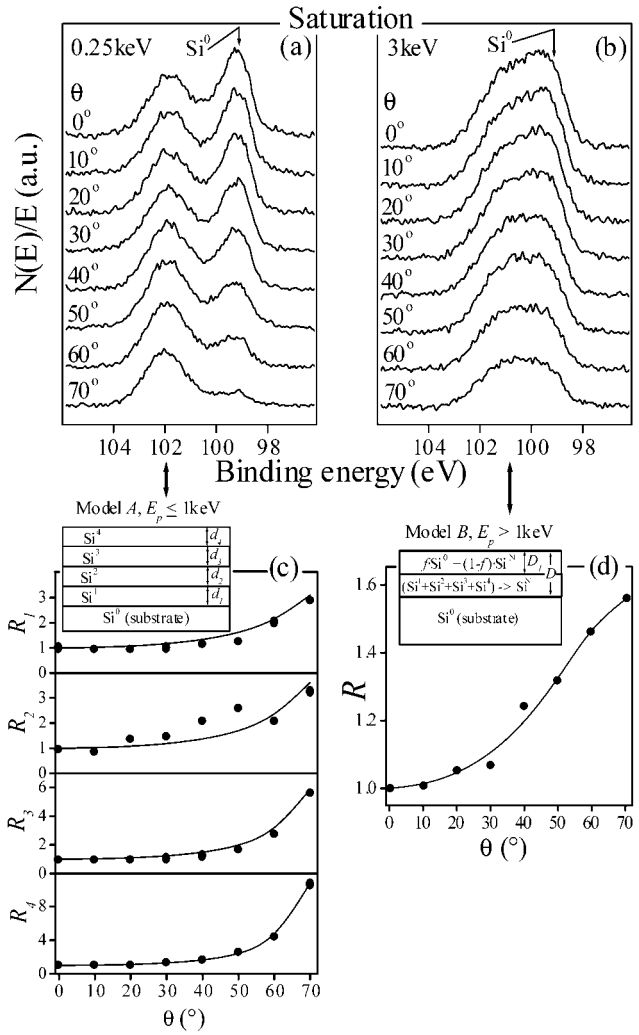

Figure 4. Si 2p XPS spectra for different takeoff angles of the nitride layer formed by N_2^+ implantation at (a) 0.25 and (b) 3 keV at the saturation dose. Intensity ratios R_1, R_2, R_3, and R_4 (panel c), and intensity ratio R (panel d) calculated as explained in the text are also shown. In addition, schematic diagrams of the parametric models used to describe the formed film at ion energies $E_p \leq 1$ keV and $E_p > 1$ keV are also included.

ion energy during N_2^+ implantation on aluminum surfaces. The above-mentioned mechanisms point to a decrease in the measured nitrogen concentration with increasing ion energy, in good agreement with results of Figure 3.

To obtain additional insight into the film composition, ARXPS was used. ARXPS is a nondestructive technique that yields quantitative in-depth information. Contrary to sputter depth profiling, any surface alteration can be excluded. ARXPS is being currently used to obtain in-depth information of films in which the thickness is of the same order of magnitude as that of the escape depth of emitted photoelectrons.[4,8] In fact, Si 2p angle-resolved photoemission studies of the SiO_2/Si(100) and SiO_2/Si(111) interfaces have been carried out to derive simple models of the in-depth distribution of the individual oxidation states of silicon (Si^{1+}, Si^{2+}, Si^{3+}, and Si^{4+}) in ultrathin silicon oxide layers.[9,13] However, to our knowledge, no similar study for SiN_x layers formed upon nitrogen implantation has been reported previously in the literature, leaving an important lack of information on the in-depth distribution of Si^n species.

Figure 4 shows the Si 2p spectra at saturation dose as a function of the takeoff angle, θ, for (a) 0.25 and (b) 3 keV ion energies. Similar sets of spectra have been measured for 0.5, 1, and 5 keV. Two different types of evolution with the takeoff angle have been observed. For $E_p \leq 1$ keV, the Si 2p spectrum shows important changes with increasing θ. The Si^0 component strongly attenuates and practically disappears at grazing angles. In contrast, for $E_p > 1$ keV, the Si 2p spectrum only presents slight changes with θ, and an important contribution of Si^0 can be observed at higher takeoff angles. According to the values of R_p and ΔR_p for Si and Si_3N_4 targets given in Table 1 and considering that the attenuation length of Si 2p photoelectrons in Si_3N_4 is ~27 Å,[14] the Si^0 contribution observed in Figure 4b and the similar one for the 5 keV SiN_x film (not shown) should disappear at higher takeoff angles. The unexpected behavior of the Si 2p ARXPS spectra for $E_p > 1$ keV can be explained by assuming the hypothesis of the formation of reduced Si^0 species at the surface as a consequence of preferential nitrogen sputtering effects and considering the increase of sputtering yield with ion energy.

Spectra of Figure 4a,b and those similar for 0.5, 1, and 5 keV ion energies have been deconvoluted into Si^0, Si^1, Si^2, Si^3, and Si^4 (see Figure 1). The takeoff angle dependence of the intensity ratios among the different Si species can be interpreted by two different models. For $E_p \leq 1$ keV, the parametric model, labeled A, has to be used. This model considers the superposition of four layers of uniform composition. A Si^4 layer on top of Si^3 followed by a layer of Si^2 on top of Si^1, of thicknesses d_4, d_3, d_2, and d_1, respectively, on top of the silicon substrate (see schematic illustration in Figure 4c). The intensities of the different Si^n species are given by eqs 2−6:

$$I(\mathrm{Si}^4(\theta)) = I^\infty(\mathrm{Si}^4)\left(1 - \exp\left(\frac{-d_4}{\lambda \cos\theta}\right)\right) \quad (2)$$

$$I(\mathrm{Si}^3(\theta)) = I^\infty(\mathrm{Si}^3)\left(1 - \exp\left(\frac{-d_3}{\lambda \cos\theta}\right)\right)\exp\left(\frac{-d_4}{\lambda \cos\theta}\right) \quad (3)$$

$$I(\mathrm{Si}^2(\theta)) = I^\infty(\mathrm{Si}^2)\left(1 - \exp\left(\frac{-d_2}{\lambda \cos\theta}\right)\right)\exp\left(\frac{-(d_3 + d_4)}{\lambda \cos\theta}\right) \quad (4)$$

$$I(\mathrm{Si}^1(\theta)) = I^\infty(\mathrm{Si}^1)\left(1 - \exp\left(\frac{-d_1}{\lambda \cos\theta}\right)\right)\exp\left(\frac{-(d_2 + d_3 + d_4)}{\lambda \cos\theta}\right) \quad (5)$$

$$I(\mathrm{Si}^0(\theta)) = I^\infty(\mathrm{Si}^0)\exp\left(\frac{-(d_1 + d_2 + d_3 + d_4)}{\lambda \cos\theta}\right) \quad (6)$$

In addition, ratios R_1, R_2, R_3, and R_4 are defined by eqs 7−10:

$$R_4 = \frac{I(\mathrm{Si}^4(\theta))/I(\mathrm{Si}^0(\theta))}{I(\mathrm{Si}^4(\theta{=}0))/I(\mathrm{Si}^0(\theta{=}0))} \quad (7)$$

$$R_3 = \frac{I(\mathrm{Si}^3(\theta))/I(\mathrm{Si}^0(\theta))}{I(\mathrm{Si}^3(\theta{=}0))/I(\mathrm{Si}^0(\theta{=}0))} \quad (8)$$

$$R_2 = \frac{I(\mathrm{Si}^2(\theta))/I(\mathrm{Si}^0(\theta))}{I(\mathrm{Si}^2(\theta{=}0))/I(\mathrm{Si}^0(\theta{=}0))} \quad (9)$$

$$R_1 = \frac{I(\mathrm{Si}^1(\theta))/I(\mathrm{Si}^0(\theta))}{I(\mathrm{Si}^1(\theta{=}0))/I(\mathrm{Si}^0(\theta{=}0))} \quad (10)$$

In eqs 2−6, $I^\infty(\mathrm{Si}^4)$, $I^\infty(\mathrm{Si}^3)$, $I^\infty(\mathrm{Si}^2)$, $I^\infty(\mathrm{Si}^1)$, and $I^\infty(\mathrm{Si}^0)$ are the intensities of infinite layers of Si,[4] Si^3, Si^2, Si^1, and Si^0,

respectively. The attenuation length of Si 2p photoelectrons through the layers $Si,^4$ Si^3, Si^2, Si^1, and Si^0 was assumed to be $\lambda \approx 27$ Å.[14]

For $E_p > 1$ keV, model B was used (see schematic illustration in Figure 4d). This model assumes a double layer for nitride film of total thickness D. The outer layer, of thickness D_1, is composed of a fraction f of Si^0 reduced species and a fraction $(1 - f)$ of a mixture of Si^1, Si^2, Si^3, and Si^4 (Si^N) species, whereas the inner layer is only composed of a mixture of Si^1, Si^2, Si^3, and Si^4 (Si^N) species. For model B, $I(Si^N)$ and $I(Si^0)$ are given by eqs 11 and 12, respectively,

$$I(Si^N(\theta)) = I^\infty(Si^N)\left[f\exp\left(\frac{-D_1}{\lambda\cos\theta}\right)\left(1 - \exp\left(\frac{-(D-D_1)}{\lambda\cos\theta}\right)\right) + (1-f)\left(1-\exp\left(\frac{-D}{\lambda\cos\theta}\right)\right)\right] \quad (11)$$

$$I(Si^0(\theta)) = I^\infty(Si^0)\left[\exp\left(\frac{-D}{\lambda\cos\theta}\right) + f\left(1-\exp\left(\frac{-D_1}{\lambda\cos\theta}\right)\right)\right] \quad (12)$$

and the ratio R is defined by eq 13.

$$R = \frac{I(Si^N(\theta))/I(Si^0(\theta))}{I(Si^N(\theta{=}0))/I(Si^0(\theta{=}0))} \quad (13)$$

The experimental ratios R_1, R_2, R_3, and R_4 for the 0.25 keV and R for the 3 keV SiN_x films are plotted in Figure 4, parts c and d, respectively, as a function of the takeoff angle (solid circles). By applying a least-squares fit between the experimental data and the models proposed by eqs 7−10 and 13 to obtain the best simultaneous fit of all curves, the thicknesses of the different layers, d_1, d_2, d_3, and d_4 for model A and D and D_1 for model B, were computed. In model B, the fraction f of Si^0 reduced species was allowed to vary between 0 and 1. The best fit is represented by the solid lines in Figure 4c,d. It corresponds to the assumption of $d_4 = 8.9 \pm 0.5$, $d_3 = 9.2 \pm 0.5$, $d_2 = 2.2 \pm 1.2$, and $d_1 = 1.9 \pm 1.2$ Å for the 0.25 keV SiN_x film and $D_1 = 15.1 \pm 1.3$ Å, $D = 33.5 \pm 2.4$ Å, and $f = 0.28 \pm 0.01$ for the 3 keV film. It is necessary to indicate that data for 0.5 and 1 keV ion energies are also perfectly fitted by model A, whereas model B is necessary for the 5 keV data.

As already pointed out, the model B proposed for $E_p > 1$ keV supports the idea of the formation of a mixed layer involving Si^1, Si^2, Si^3, and Si^4 species, with the presence of Si^0 reduced species at the near surface. The formation of a mixture of Si^1, Si^2, Si^3, and Si^4 species should be attributed to knock-on mechanisms, which are enhanced with increasing ion energies and would lead to the mixing of all Si species in a single layer. On the other hand, the formation of Si^0 reduced species at the surface can be explained assuming the superposition of two mechanisms: nitridation and nitrogen removal. Nitridation occurs largely for low and intermediate ion doses. With increasing the ion dose, the nitrogen removal process starts to compete with the nitridation process leading to a steady state at saturation. According to the sputtering yield values of Table 1, the nitrogen removal should be attributed to preferential sputtering of nitrogen in such a way that a layer containing Si^0 reduced species of thickness roughly equal to ΔR_p is formed at the surface. For $E_p \leq 1$ keV, neither preferential sputtering nor knock-on effects would be sufficiently important to compete with the nitridation process and a layered film composed of four transition layers is formed. It is worthy to note that the model explaining the nitride film growth for $E_p \leq 1$ keV is similar to that proposed to explain the SiO_2/Si(100) interface formed by exposing a clean Si(100) substrate to pure oxygen.[9] It must be also pointed out that this model is idealized. In reality, concentration gradients rather than sharp boundaries are to be expected in the film. However, this is the simplest model compatible with the experimental results.

Conclusions

The formation of silicon nitride by low-energy N_2^+ beams has been investigated. The results show that N_2^+ beams in the range 0.25−5 keV react with Si to produce SiN_x surface films. The nitride concentration depth profiles were obtained from the ARXPS measurements using parametric models. It was observed that the concentration depth profiles are dependent on the N_2^+ energy. For energies below 1 keV, the SiN_x surface film can be modeled by a layered film in which the composition is $Si,^4$ Si^3, Si^2, and Si^1 in going from the surface to the substrate. For energies above 1 keV, a nitride film composed of a mixture of Si^1, Si^2, Si^3, and Si^4 species with reduced Si^0 species at the near surface was found. The differences are attributed to preferential sputtering of nitrogen and knock-on effects, which become more important as the energy increases.

Acknowledgment. The authors thank D. Díaz for technical assistance. This work was financially supported by the Spanish Comisión Interministerial de Ciencia y Tecnología (Project MAT99-0830-C03-02).

References and Notes

(1) Morosanu, C. E. *Thin Solid Films* **1980**, *65*, 171.
(2) Kärcher, R.; Ley, L.; Johnson, R. L. *Phys. Rev. B* **1984**, *30*, 1896.
(3) Baek, D. H.; Kang, H.; Chung, J. W. *Phys. Rev. B* **1994**, *49*, 2651.
(4) Palacio, C.; Gómez-Aleixandre, C.; Díaz, D.; García, M. M. *Vacuum* **1997**, *48*, 709.
(5) Taylor, J. A.; Lancaster, G. M.; Ignatiev, A.; Rabalais, J. W. *J. Chem. Phys.* **1978**, *68*, 1776. Taylor, J. A. *Appl. Surf. Sci.* **1981**, *7*, 168.
(6) Kusunoki, I.; Takaoka, T.; Igari, Y.; Ohtsuka, K. *J. Chem. Phys.* **1994**, *101*, 8238.
(7) Hasegawa, S.; Zalm, P. C. *J. Appl. Phys.* **1985**, *58*, 2539.
(8) Palacio, C.; Arranz, A. *J. Phys. Chem. B* **2000**, *104*, 9647.
(9) Oh, J. H.; Yeom, H. W.; Hagimoto, Y.; Ono, K.; Oshima, M.; Hirashita, N.; Nywa, M.; Toriumi, A.; Kakizaki, A. *Phys. Rev. B* **2001**, *63*, 205310.
(10) Proctor, A.; Sherwood, M. P. A. *Anal. Chem.* **1982**, *54*, 13.
(11) Ziegler, J. F.; Biersack, J. B.; Littmark, U. *The Stopping and Range of Ions in Matter*; Pergamon: New York. 1985; Vol. 1. SRIM-2000©, Ziegler, J. F., 1201 Dixona Drive/Edgewater, MD, 21037, USA, http://www.SRIM.org.
(12) Taylor, J. A.; Rabalais, J. W. *J. Chem. Phys.* **1981**, *75*, 1735.
(13) Luh, D. A.; Miller, T.; Chiang, T. C. *Phys. Rev. Lett.* **1997**, *79*, 3014.
(14) Tanuma, S.; Powell, C. J.; Penn, D. R. *Surf. Interface Anal.* **1991**, *17*, 911, 927.